Soil Deformation Monitoring System using Soil Vibration and Moisture Sensors

Yakobus Yulianto Kevin, Erwin Susanto and Husneni Mukhtar
Telkom University, Jl. Telekomunikasi Terusan Buah Batu, Bandung, Indonesia

Keywords: Landslide Monitoring System, Geophone Sensor, Soil Moisture Sensor, Zigbee

Abstract: Landslides are natural disasters that often occur in Indonesia. In 2018 474 landslides in Indonesia resulted in many fatalities and many damaged buildings. To minimize losses caused by landslides, a tool for monitoring the soil condition is needed. In this research, sensors of soil vibration and soil moisture were utilized to develop a monitoring system of soil deformation that was able to perform continuously in real-time. For the data transfer, the Zigbee module, as wireless data communication, sent the acquired data from both sensors to Antares as an IoT platform via node-MCU ESP8266. The monitoring simulation of the soil deformation was carried out on a plant prototype placed indoors by embedding a spring on all four corners or feet of the plant prototype. Results of this monitoring system were displaying the vibration and moisture data of soil condition is continuous and real-time. The vibration data from the geophone sensor with 99.97% of sensor accuracy were sent to the IoT platform and displayed on the monitor. While the moisture sensor (soil moisture v1.2) with 99.71% of average accuracy. The communication system sending data from the sensor to Antares produces an average delay of 2.3 seconds.

1 INTRODUCTION

Indonesia is one of the countries prone to natural disasters globally because it has a geographical condition that consists mainly of mountains, hills, valleys, and vast seas. One of the natural disasters that often occurs in Indonesia is landslides. A landslide is a geological event that occurs due to rock or soil mass movement with various types and types, such as falling rocks or large lumps of soil. According to the National Disaster Management Agency (BNBP) in Indonesia, in 2018, 474 landslide incidents in Indonesia resulted in many fatalities and many damaged buildings. Landslides usually occur in mountainous areas, hills, steep slopes, or cliffs. The cause of landslides is high rainfall, deforested forests, not dense soil and small vibrations caused by vehicle traffic around the hillsides. Due to the frequent occurrence of landslides, we need a monitoring system of ground movement in a particular area. This system is that it can monitor the condition of ground movement continuously in real-time.

Some previous research reports on landslide warning system can be found, for example, is the Landslide Warning System on the Railroad Track (Hartalita, et al., 2018). This study used an accelerometer sensor ADXL345 with the advantage of detecting the tilt and converting it to angular degrees with a sensor accuracy of 96.45%. The drawback of this sensor is that it cannot follow fast movements due to its slow response. The other report uses light sensors, i.e., light-dependent resistor (LDR), to detect landslide events (Sudibyo, Herawadi, 2015). The advantage of this sensor is that it can read ground motion by utilizing light. The drawback is that the error value obtained from the measurement is about 5%.

Landslide detection using ultrasonic and infrared with short message service (SMS) notification was reported in (Widhiantoro and Purwarupa, 2015). The advantage of the infrared sensor is that it can detect the existence of moving objects such as humans and animals and soil movements. In contrast, the ultrasonic sensor can be used to detect their movements. The disadvantage is that if the ground movement is less than 2 cm, the sensor cannot read the variations accurately. In this paper, we use a vibration sensor and humidity sensor to monitor ground motion. Then the data is processed and displayed as information on the condition of soil movement.

Kevin, Y., Susanto, E. and Mukhtar, H.
Soil Deformation Monitoring System using Soil Vibration and Moisture Sensors.
DOI: 10.5220/0010797100003317
In *Proceedings of the 2nd International Conference on Science, Technology, and Environment (ICoSTE 2020) - Green Technology and Science to Face a New Century*, pages 117-124
ISBN: 978-989-758-545-6

2 RESULTS AND DISCUSSION

2.1 Basic Theory

2.1.1 Geophone Sensor

A geophone principle work is the conversion of ground motion (displacement) into voltage. Zan et al. deployed a geophone to sense the landslide early warning system (Zan, et al., 2002). Many types of vibration signals induced by traffic, train movement or regular tapping can be sensed by a geophone (Kunnath, et al., 2010). Geophone has two main components, namely permanent magnets and wire windings, shown in Figure 2.1.

Figure 2.1. Main Components of Geophones

Geophone works based on Faraday's law, where the magnetic flux variations cause the electric current flow in a coil in varied times. The magnitude of the stress on a geophone that occurs is directly proportional to the flux changes concerning time. Faraday's Law can be stated by the formula below:

$$\varepsilon = -N(\Delta\Phi/\Delta t) \quad (1)$$

where
ε = induced GGL (volts),
N = Number of coil windings
ΔΦ = Change in magnetic flux (weber)
Δt = time-lapse (s)
The negative sign indicates the direction of the induced electromotive force (emf).

2.1.2 High Pass Filter

High Pass Filter (HPF) is a filter or frequency filter that can pass high-frequency signals and inhibit or block low-frequency signals or frequencies under cut-off frequencies. To determine the value of the cut-off frequency, it can be calculated using the formula:

$$f_c = \frac{1}{2\pi RC} \quad (2)$$

where:
f_c = Cut off frequency in units of Hz
π = 3.14
R = Resistance in Ohms (Ω)
C = Capacitance in Farad (F)

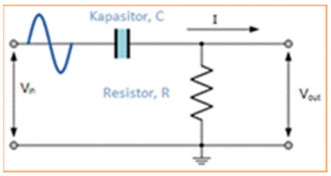

Figure 2.2. High Pass Filter Circuit

2.1.3 ADS1115 Module

ADS1115 module is a type of ADC with a 16-bit resolution with a high level of conversion accuracy compared to the 10-bit ADC. In this ADC, four channels can convert values for four sensors simultaneously with bipolar or single differentials. The received data will be transferred or sent via I2C serial communication. The series consists of SDA and SCL. The next Figure 2.3 shows the ADS1115 module.

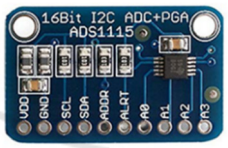

Figure 2.3. *ADS1115 Module*

2.1.4 Soil Moisture Sensor

A soil moisture sensor is a sensor that can detect moisture in the soil. This sensor consists of two parts, namely the probe and the comparator. In the comparator part, there is an IC TLC555I that serves as a voltage comparator. At the same time, the probe has a function to pass current through the ground and read the resistance proportional to the value of the humidity level. Measurement of soil moisture can be done by the relations of mass of water MA, the mass of wet soil MTB, the mass of dry soil MTK and soil moisture KT (Stevanus and Setiadi, 2013):

$$MA = MTB - MTK \quad (3)$$

$$KT = (MA/MTB) \times 100\% \quad (4)$$

Figure 2.4. Soil Moisture Sensor

Many usages of soil moisture sensors can be found in real applications such as to monitor sports turf humidity, especially for a golf game, to reveal

ancient irrigation practices in waterless environment, etc.

People monitor soil moisture for many beneficial for environmental researchers and practitioners like farmers, golf course superintendents, archaeologists, and regulators (Kumar, et al., 2016).

2.1.5 Zigbee

RF transceiver modules are set in Digi XBee S2C to provide wireless connectivity using the Zigbee protocol. The configuration consists of XCTU for the connection of coordinator and router using AT commands and MAC addresses. The coverage of the connection is 60 m indoor and 1200 m outdoor.

Figure 2.5. Zigbee

2.1.6 Arduino Uno

We use Atmega328 Arduino microcontrollers with an open-source physical computing platform. It contains 20 I/O pins, 14 digital and six analogue pins, a 16 MHz crystal oscillator, a Universal Serial Bus (USB) connection, a power jack, an ICSP header and a reset button as shown in Figure 2.6. To embed programs in Arduino boards, USB-to-serial adapter chips such as the FTDI FT232 can be employed.

Figure 2.6. Arduino Uno

2.1.7 Node MCU ESP 8266

NodeMCU ESP8266 is an embedded microcontroller system equipped with Wi-Fi intact. Therefore, it does not need to use additional Wi-Fi devices. The system architecture is on the chip (SoC) and has a function for communicating GPIO by connecting and transmitting data through the Internet. Figure 2.7 shows the I / O pins of NodeMCU (Shkurti, 2017).

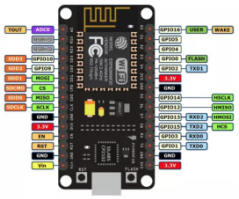

Figure 2.7. NodeMCU ESP 8266

The standard Lua Programming firmware script was often used to simplify programming, and it usually needs the existing library in the Arduino IDE software. This software is open and can be downloaded and run well in the operating system (Prayogo and Suryo, 2016).

2.2 System Design

2.2.1 Hardware Design

A block diagram of a deformation monitoring system of ground motion using a geophone sensor and a soil moisture sensor is shown in Figure 3.1.

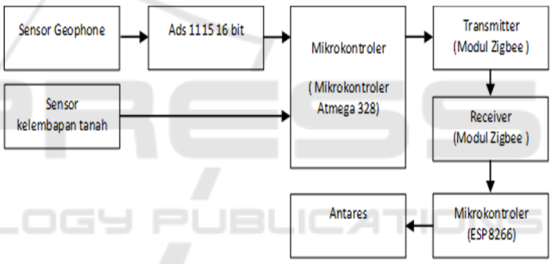

Figure 3.1. Block Diagram

To monitor the ground motion deformation using a geophone sensor and a soil moisture sensor is to conduct a two-season trial, namely the dry and rainy seasons. During the dry season, the signal level generated from the soil moisture sensor does not experience any significant changes because the humidity in the soil tends to be more stable. Meanwhile, soil conditions tend to be wet during the rainy season to increase the humidity sensor output measurement. Unlike the soil moisture sensor, the level generated by the ground vibration sensor tends not to be affected by seasonal changes. The geophone sensor will display a significant change only when getting vibration.

2.2.2 Software Design

Figure 3.2 shows a flowchart that illustrates the algorithm of a soil deformation monitoring system using a geophone sensor and a soil moisture sensor.

The first step that must be done is to initialize the geophone sensor input and the soil moisture sensor. Inputs generated by geophone sensors and soil moisture sensors are analogue signals which the ADC port will then process on the microcontroller to convert the analogue voltage to digital voltage. After that, the Atmega 328 microcontroller will read the input provided by the sensor. The output signal from the Atmega 328 Microcontroller will be forwarded to the transmitter part of the Zigbee module to be sent to the receiver part of the Zigbee module. The signal data that the receiver has received will be forwarded to the Antares using nodeMCU ESP8266 to be displayed in graphical form.

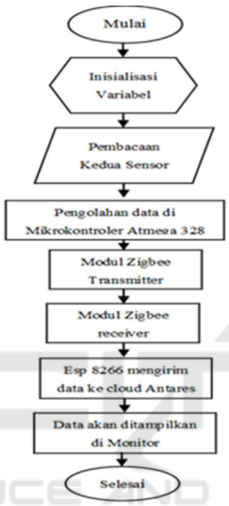

Figure 3.2. Software Design Flow Chart

2.2.3 Mechanical Design

In Figure 3.4, we can see that mechanical design aims to provide a general picture of the equipment to be tested.

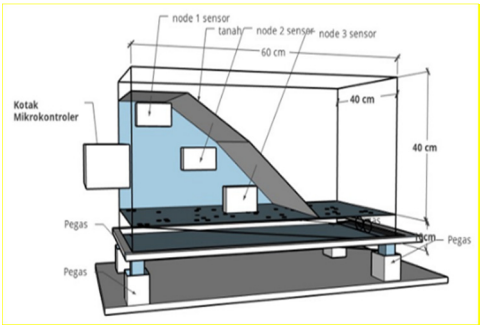

Figure 3.3. Mechanical Design

The material used to make the simulation box is transparent acrylic. The size of the simulation box is 60 cm long, 40 cm wide and 40 cm high. The box was filled with land that is set close to the actual situation. Soil moisture sensor is installed in separated 3 sensor modules while geophone sensors are installed in two places, namely sensor module 1 and sensor module 3. Each sensor module is installed with a distance of 5 cm.

2.3 Test and Analysis Results

2.3.1 Testing the Geophone Sensor

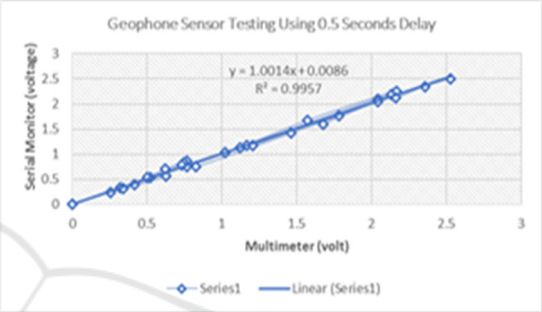

Figure 4.1. Linear Regression Chart Using a 0.5 Seconds Delay

Based on geophone sensor testing in Figure 4.1, 30 data were taken in the testing mechanism at 0.5-second intervals. The minimum output voltage is 0 volts for less vibration. In contrast, in the under-vibration state, the maximum voltage of the multimeter is 2,528 volts, and it equals 2.5 volts on the serial monitor display. Based on Figure 4.1, the formula of linear regression can be obtained using an interval of 0.5:

y=1,0014x+00,086

2.3.2 Moisture Sensor Testing

Table 4.1. Soil Moisture Sensor Testing

Trial to	Soil Moisture Value (%)			Reference Value
	Sensor 1	Sensor 2	Sensor 3	
1	100	99.71	99.69	100
2	100	99.42	99.38	100
3	100	99.71	99.38	100
4	100	99.71	99.07	100
5	100	100	99.38	100
6	100	99.71	99.38	100
7	100	100	99.38	100
8	100	100	99.38	100
9	100	99.71	99.38	100
10	100	100	99.07	100
Avg	100	99.797	99.349	100

From the experiment results in Table 4.1, the mean of sensor measurements is 100% (sensor 1), 99.80% (sensor 2) and 99.35% (sensor 3).

2.3.3 Zigbee Testing

- Delay Testing

The following is the experiment result of delay testing of Zigbee in tabular form.

Table 4.2. Zigbee Test Results

Data delivery interval (seconds)	Average Delay (seconds)			
	Horizontal Testin		Vertical Testing	
	Indoor 3.5 m	Outdoor 10 m	Height of 3,5 m	Height of 7 m
1	1,258	3,175	3,985	2,868
2	1,120	1,677	2,839	3,281
3	0,993	1,861	2,014	3,682
4	1,102	1,423	1,577	2,721
5	1,531	1,816	1,918	2,290
10	0,992	1,692	0,517	0,693
15	1,029	1,944	0,514	0,947
20	0,992	2,252	0,503	0,761
25	1	2,268	0,544	1,008
30	0,994	1,754	0,508	1,029

From the data testing results, it can be concluded that the value at intervals of 1,2,3,4 and 5 seconds delay is greater than the interval values of 10, 15, 20, 25 and 30 seconds. Moreover, at the 10-second interval, the resulting data is better than other intervals.

- Testing Data Loss

Table 4.3. Zigbee Data Loss Testing Results

Data delivery interval (sec)	Average Data Loss (%)			
	Indoor 3.5 m	Outdoor 10 m	Height of 3,5 m	Height of 7 m
1	0	7,196	38,557	0
2	0	1,685	16,176	5,747
3	0	1,667	5,217	38,970
4	0	0	0	10,416
5	0	18,072	40,740	0
10	0	0	0	0
15	0	21,67	0	6,67
20	0	10	0	0
25	0	11,67	0	5
30	0	5	0	15

Based on tests conducted, it can conclude that the 4s interval is suitable because it has the slightest delay compared to other intervals.

2.3.4 Testing Data Transmission to the Cloud

- Delay Testing

Table 4.4 Testing Delay from NodeMCU ESP8266 to Antares

Interval (seconds)	Average delay (ms)
1	598
2	329
3	513
4	317
5	407
6	405
7	473
8	475
9	458
10	465

Based on tests conducted, it can conclude that the 4s interval is suitable because it has the slightest delay compared to other intervals.

- Data Loss Testing

Table 4.5. Testing Data loss from NodeMCU ESP8266 to Antares

Interval (seconds)	*Data* Loss (%)
1	0
2	0
3	0
4	0
5	0
6	0
7	0
8	0
9	0
10	0

Based on Table 4.6, it can be seen that in conducting data transmission trials, there was no data loss found in data transmission.

- Overall Sensor Testing

This experiment uses two geophone sensors and three soil moisture sensors. The node 1 geophone sensor is installed at the top of the landslide, and the node 3 geophone sensor is installed at the bottom of the landslide while the humidity sensor is placed in the ground part of node 1, node 2 and node 3.

Testing scenario:

First, all data were taken randomly to determine the value of humidity and vibration values during initial

conditions. During 13 minutes, the box simulation is vibrated twice. After 13 minutes, the researchers experimented from dry to wet by spraying as much as 1 litre of water to replace rain. After 13 minutes, the researchers vibrated five times randomly. After that, the researchers conducted an experiment from wet to dry, namely, installing two light bulbs to dry the soil. The soil drying process lasts for an entire night. After that, the researchers conducted another five random vibrations. The following results are graphs of the vibration sensor and soil humidity during dry, dry to wet and wet to dry conditions.

- Dry Conditions

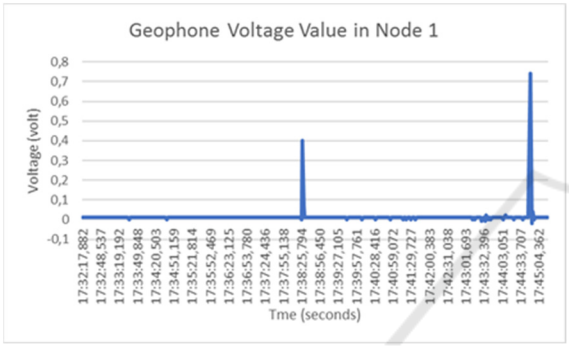

Figure 5.1. Graph of Geophone Voltage Values in Node 1 During Dry Conditions

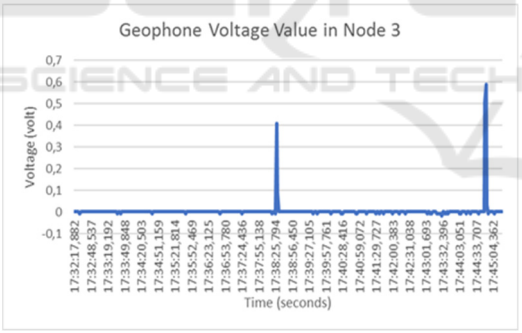

Figure 5.2. Graph of Geophone Voltage Values in Node 3 during dry conditions

In the two graphs above, the artificial vibrations are made to 2 vibrations so that the two geophone sensors detect these vibrations.

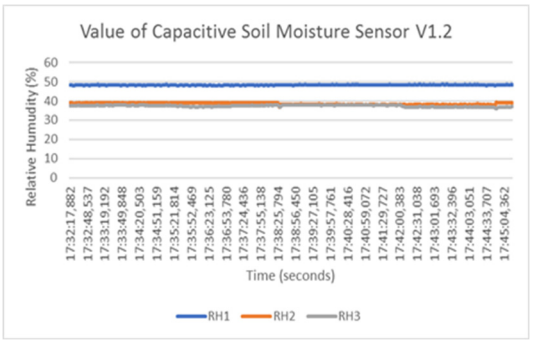

Figure 5.3. Capacitive Soil Moisture Sensor V1.2, during dry conditions

Based on the graph above, when conditions are dry, the geophone sensor detects two artificial vibrations. It can conclude that the vibration created does not affect the soil moisture level.

- Dry to Wet Conditions

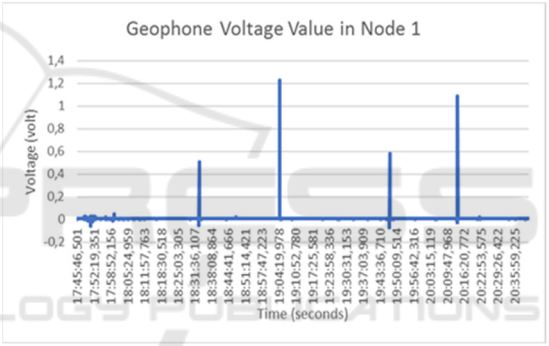

Figure 5.4. Graph of Geophone Voltage Value in Node 1 during dry to wet

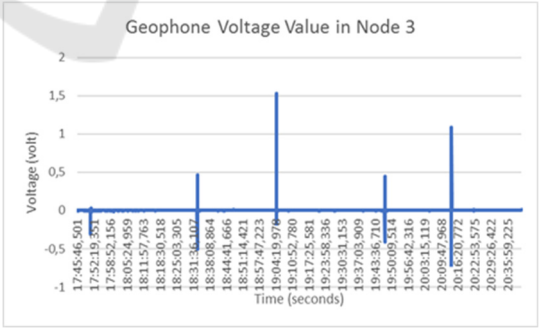

Figure 5.5. Geophone Voltage Value Charts in Node 3 during dry to wet

When conditions are dry to wet, the number of artificial vibrations is carried out by five vibrations at random, and the geophone sensor in node 1 detects a total of 4 vibrations. In comparison, in node three, the artificial vibrations detected amounted to 5

vibrations. The geophone sensor at node three is installed at the bottom of the landslide so that it is faster and more sensitive when it receives vibrations.

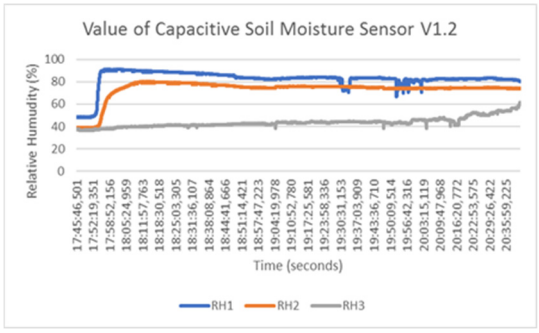

Figure 5.6. Capacitive Soil Moisture Sensor V1.2 Graph When Dry to Wet Conditions

Based on the capacitive soil moisture sensor v1.2 chart, the sensor value at nodes 1 and 2 has a good increase. In contrast, sensor 3 has a rate increase due to the location of sensor three at the bottom of the soil, so that it takes a long time for water to seep into the ground and detect by sensors. In the soil moisture sensor graph, a dashed line indicates that the geophone sensor is detecting the vibration at that time. The test results from dry to wet conclude that the change in soil moisture does not affect the ground vibration, of the voltage generated by the ground vibration sensor is relatively the same.

- Wet to Dry Condition

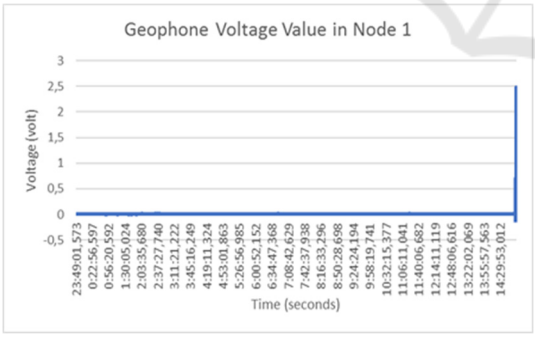

Figure 5.7. Geophone Voltage Value Charts in Node 1 during wet to dry

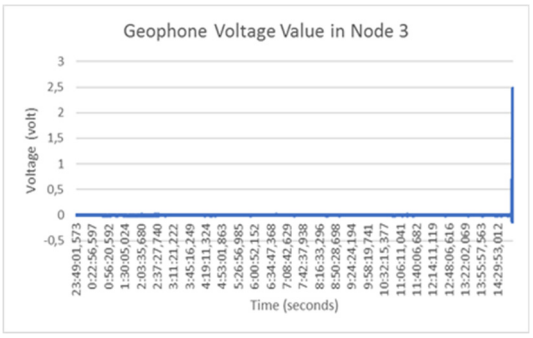

Figure 5.8. Geophone Voltage Value Chart in Node 3 when during wet to dry

In Figure 4.8 and Figure 4.9 both geophones experience the same increase in voltage. There was an increase in voltage because, at that time, researchers conducted artificial vibrations.

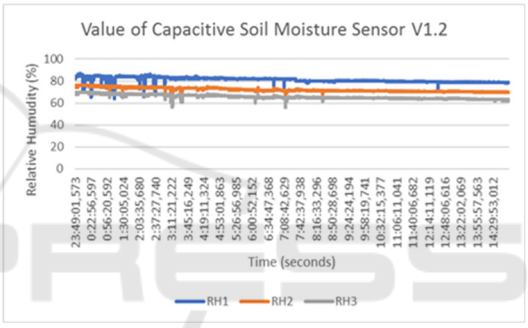

Figure 5.9. Capacitive Soil Moisture Sensor V1.2 Graph during wet to dry

The graph above can conclude that the three sensors can function well and experience a slight decrease in per cent humidity. In the graph of capacitive soil moisture sensor V1.2, there is a dotted line indicating that the geophone sensor detects the vibration at that time.

REFERENCES

A. Hartalita, A. Sugiana, A. Rusdinar, 2018, Sistem Peringatan Tanah Longsor pada Jalur Kereta Api, *e-Proceeding of Engineering*, Vol. 5, No., 3, pp. 4301-4307.

BNPB, *Data Bencana Tanah Longsor 2018*, available at http://bnpb.cloud/dibi/laporan4, 4 February 2019.

D. Widhiantoro, Purwarupa, 2015, Sistem Pendeteksi Tanah Longsor Menggunakan Ultrasonik Dan Infrared dengan Notifikasi SMS, *Jurnal Kajian Teknik Elektro*, Vol. 1, No. 2.

Kumar, Matti Satish, Pradeep Kumar, Ritesh Chandra, Sabarimalai Manikandan, 2016, Monitoring moisture

of soil using low cost homemade Soil Moisture Sensor and Arduino UNO, *ICACCS 2016 IEEE International*.

Kunnath, Abishek Thekkyil, Ramesh, Menemsha Vinodini, 2010, Integrating Geophone Network to Real-Time Wireless Sensor Network System for Landslide Detection, *SENSORDEVICES*, IEEE International, pp.167-171.

L. Shkurti, 2017, Development of Ambient Environmental Monitoring System Through Wireless Sensor Network (WSN) Using NodeMCU and WSN Monitoring, *The 6th Mediterranean Conference On Embedded Computing*.

L. Zan, G. Latini, E. Piscina, G. Polloni, and P. Baldelli, 2002, Landslides Early Warning Monitoring System, Geoscience and Remote Sensing Symposium, *IGARSS 2002*, IEEE International, Vol 1, pp. 188-190.

Prayogo, Sandy Suryo, 2016, The Use and Performance of MQTT and CoAP as Internet of Things Application Protocol using NodeMCU ESP8266, *ICIC*, IEEE International.

Stevanus, Setiadi, K.. D., 2013, Alat Pengukur Kelembaban Tanah Berbasis Mikrokontroler Pic 16f84, Jurnal Teknik Elektro Universitas Kristen Maranatha, Vol. 3, No. 1.

Sudibyo, Novi Herawadi, 2015, Pendeteksi Tanah Longsor Menggunakan Sensor Cahaya, *Jurnal Teknologi Informasi Magister*, Vol. 1, No. 2.